Food Chemistry 174 (2015) 621–629

Contents lists available at ScienceDirect

Food Chemistry

journal homepage: www.elsevier.com/locate/foodchem

Isolation and characterisation of sericin antifreeze peptides and molecular dynamics modelling of their ice-binding interaction

Jinhong Wu [a], Yuzhi Rong [a], Zhengwu Wang [a], Yanfu Zhou [b], Shaoyun Wang [b,*], Bo Zhao [c]

[a] Department of Food Science and Engineering, Bor S. Luh Food Safety Research Center, School of Agriculture and Biology, Shanghai Jiao Tong University, Shanghai 200240, China
[b] Department of Food Science, College of Biological Science and Technology, Fuzhou University, Fuzhou 350002, China
[c] College of Chemistry and Materials Science, Nanjing Normal University, Nanjing 210097, China

ARTICLE INFO

Article history:
Received 13 May 2014
Received in revised form 21 October 2014
Accepted 17 November 2014
Available online 23 November 2014

Keywords:
Sericin peptides
Antifreeze activity
Isolation
Ice-binding
Molecular dynamic modelling

ABSTRACT

This study aimed to isolate and characterise a novel sericin antifreeze peptide and investigate its ice-binding molecular mechanism. The thermal hysteresis activity of ice-binding sericin peptides (I-SP) was measured and their activity reached as high as 0.94 °C. A P4 fraction, with high hypothermia protective activity and inhibition activity of ice recrystallisation, was obtained from I-SP, and a purified sericin peptide, named SM-AFP, with the sequence of TTSPTNVSTT and a molecular weight of 1009.50 Da was then isolated from the P4 fraction. Treatment of *Lactobacillus delbrueckii* Subsp. *bulgaricus LB340 LYO* with 100 μg/ml synthetic SM-AFP led to 1.4-fold increased survival ($p < 0.05$). Finally, an SM-AFP/ice binding model was constructed and results of molecular dynamics simulation suggested that the binding of SM-AFP with ice and prevention of ice crystal growth could be attributed to hydrogen bond formation, hydrophobic interaction and non-bond interactions. Sericin peptides could be developed into beneficial cryoprotectants and used in frozen food processing.

1. Introduction

Antifreeze proteins (AFPs) are commonly referred to as thermal hysteresis proteins, or ice-structuring proteins. AFPs are a family of polypeptides that have thermal hysteresis ability (THA), which lowers the freezing temperature of body fluids via a noncolligative mechanism without changing the melting point significantly. They also have the recrystallisation inhibition (RI) ability, which inhibits the growth of ice in an adsorption-inhibition mechanism by binding to the ice surface (Jia et al., 2012). These unique functions of AFPs have attracted significant interest for their potential applications in the food, medical, and agricultural industries where low temperature storage is required and ice crystallisation is damaging. Typical applications of AFPs include improving the smoothness and texture of frozen foods, the preservation of cell lines, organs, and cryosurgery, and the development of cold-adapted transgenic plants and animals (Venketesh & Dayananda, 2008).

AFPs with remarkably diverse structures have been discovered in many cold-adapted organisms, including fish, plants, bacteria, and insects (Cheng, 1998; Xiao et al., 2010). For example, four classes of structurally diverse AFPs were identified in the body fluids of many species of polar fish (Harding, Anderberg, & Haymet, 2003). Similarly, many species of perennial winter plants expressed AFPs with strong ice RI activity in their seeds, stems, buds, crowns, leaf blades, flowers, berries, and roots (Venketesh & Dayananda, 2008), whereas bacterial AFPs, with high antifreeze activity, were isolated from six out of 82 bacterial strains at Ross Island in the McMurdo Dry Valleys region of Antarctica (Kawahara, 2002). AFPs from insects, such as the beetle and spruce budworm, had the unique feature that they were 10–100 times more active than were AFPs from fish, which allowed them to survive in much colder environments (Graether et al., 2003; Graham, Qin, Lougheed, Davies, & Walker, 2007). Despite these numerous structural and functional studies, the molecular ice-binding mechanism of AFPs remained controversial until recently, when computational modelling technology was successfully used to theoretically define the antifreeze mechanism of AFPs (Hassas-Roudsari & Goff, 2012). Recently, the effect of peptides on the growth of ice crystals was demonstrated, using molecular dynamics simulations, which suggested that short peptides could also be effective antifreeze agents (Kim, Damodaran, & Yethiraj, 2009).

Recently, insect AFPs were isolated, cloned, and expressed. These novel insect AFPs had definite advantages when compared with other sources of AFPs for some industrial and biomedical purposes that involve thermal processing (Qin & Walker, 2006). Silkworms are *Lepidoptera* insects whose cocoons provide mechanical protection during the freezing of surrounding water and its expansion into

* Corresponding author. Tel./fax: +86 591 22866375.
E-mail address: shywang@fzu.edu.cn (S. Wang).

http://dx.doi.org/10.1016/j.foodchem.2014.11.100
0308-8146/

ice (Danks, 2004). Sericin, a globular and sticky protein, derived from the outer sticky layer of a silkworm cocoon, exhibits potential as a cryoprotective agent for use either in cells or with enzymes (Tsujimoto, Takagi, Takahashi, Yamada, & Nakamori, 2001). However, it is unclear how sericin may prevent inoculative freezing by isolating the integument from ice crystals, on the cocoon surface or its surroundings, in nature. Moreover, few studies about the antifreeze activity and structural characterisation of sericin have been reported. Recent studies from our laboratory suggested that sericin peptides protected against freeze-induced denaturation of grass carp surimi, and exerted cryoprotective effects on *Lactobacillus delbrueckii* Subsp. *bulgaricus LB340 LYO* during frozen storage (Wu, Wang, Wu, & Wang, 2012; Wu et al., 2013). These findings indicated that sericin peptides (SPs) could be valuable novel antifreeze peptides in industrial applications. The present study was carried out to isolate and characterise the antifreeze sericin peptide from sericin hydrolysates. Furthermore, we assessed the possible binding of purified sericin peptide to the surface of ice by molecular modelling, to further investigate the antifreeze mechanism of silkworm AFPs derived from sericin hydrolysates.

2. Materials and methods

2.1. Materials

Hydrolysed sericin peptide (SP) powder was obtained from Huzhou Xintiansi Bio-Tech Co., Ltd. (Huzhou, China). *Lactobacillus delbrueckii* Subsp. *bulgaricus LB340 LYO* (*L. bulgaricus LB340*) was purchased from Danisco (CN) Holding Co., Ltd. (Shanghai, China). M17 broth was purchased from Hopebio-Technology Co., Ltd. (Qingdao, China). The C18 reversed-phase high performance liquid preparative chromatography column (25 × 250 mm, 5 μm) was purchased from Grace Trading (Shanghai) Limited Company (Shanghai, China). The Lowry protein assay kit was purchased from Shanghai Solarbio Bioscience & Technology Co., Ltd. (Shanghai, China). All other reagents were of analytical grade.

2.2. Extraction of ice-binding sericin peptides (I-SP) by ice affinity absorption

In this study, a newly assembled ice absorption apparatus, proposed in our previous study, was used to extract I-SP, based on ice affinity absorption. The extraction process was performed under the optimal extraction conditions at a temperature of −3 °C, an original hydrolysed sericin peptide concentration of 5 mg/ml, and an extraction time of 3 h (Wu et al., 2013).

2.3. Isolation of I-SP by reversed-phase fast protein liquid chromatography

An aliquot of 2 ml of ice-binding extract, at a concentration of 20 mg/ml was loaded onto a C18 reversed-phase chromatography column (25 mm diameter × 250 mm length). The HPLC system (AKTA Purifier 100 FPLC System, GE Company, Niskayuna, NY, USA) was operated isocratically with a flow rate of 10 ml/min at room temperature, and the UV detector was set at 220 nm. The column was equilibrated with 5% acetonitrile for 5 min after injection, and the peptides were then eluted in a linear gradient of 5–90% acetonitrile for 20 min. Separated fractions were collected, and their antifreeze activities were studied.

2.4. Assaying the hypothermia protection activity of sericin peptides

The hypothermia protection activity of sericin peptides on *L. bulgaricus LB340* was assayed according to our previously described experimental protocol (Wu et al., 2013) with minor modifications. Briefly, *L. bulgaricus LB340* was revived in M17 broth for 12 h at 37 °C, 180 r/min. Fifty microlitres of seed culture media ($OD_{600} \geqslant 1.3$) were subcultured in glass tubes mixed with 4 ml of media at a 1:80 (v/v) dilution for 4 h. The *L. bulgaricus LB340* strain cells ($OD_{600} \geqslant 1.2$) were then treated with a 10^3-fold serial dilution made with sterile water. Fifty microlitres of the diluted bacterial suspension were transferred to a 2 ml cryovial, and 50 μl of sericin peptide were added and mixed by vortexing. Sterile water was used as a negative control, and 5% (v/v) glycerol as the positive control. These sample cryovials were frozen at −20 °C for 24 h. After storage, the samples were thawed at 37 °C for 10 min, and 50 μl of each sample were revived in 4 ml of M17 broth media for 7 h. The absorbance at 600 nm was then measured.

The spectrophotometric determination curve, showing the relationship between the surviving cell content and the optical density of cells at 600 nm, was obtained, and the curvilinear relationship is depicted in Eq. (1).

$$y = 0.2152\ \mathrm{Ln}(x) + 0.0594 \quad (R^2 = 0.9972) \tag{1}$$

where y is the OD_{600} of the cell suspension after 7 h of cultivation, and x is the content of viable cells of the mixed samples.

The percentage of surviving *L. bulgaricus LB340* cells, before and after frozen storage at −20 °C, was calculated using Eq. (2):

$$\text{Survival rate } (\%) = \frac{C}{C_0} \times 100 \tag{2}$$

where C_0 and C were the contents of viable cells in the samples before and after frozen storage, respectively.

The hypothermia protection activity of sericin peptides on the *L. bulgaricus LB340* was evaluated by assessing the percentage of surviving cells.

2.5. Thermal hysteresis activity analysis by differential scanning calorimetry (DSC)

The antifreeze activity of sericin peptides was also assessed, using a Netzsch 204 F1 DSC device equipped with Proteus Thermal Analysis software (Netzsch. GmbH, Selb, Germany), based on the method of Zhang, Zhang, Wang, Zhang, & Yao (2007) with minor modifications. The calorimeter was temperature- and heat-calibrated, using indium as a standard, and BSA was used as a non-antifreeze standard protein (AFP-free) to compare solutions with and without sericin antifreeze peptides. A 5 μl aliquot of sample, at a concentration of 5 mg/ml was sealed in a pre-weighed aluminium pan and cooled from room temperature to −25 °C at rate of 1 °C/min. It was then held at −25 °C for 5 min, and heated to 10 °C at a rate of 1 °C/min. The melting point (T_m) and enthalpy of melting (ΔH_m) were calculated from the DSC curve. Then, the sample was cooled from 10 to −25 °C at rate of −1 °C/min, held for 5 min, and then heated to the holding temperature (T_h) when the system was at phase-equilibrium with the solid (ice crystal) and liquid (aqueous solution). To allow for ice-antifreeze peptide interactions and system stabilisation, the sample was held at the T_h temperature for 5 min. It was then re-cooled at the same rate of −1 °C/min to −10 °C, during which the onset temperature (T_0) of crystallisation was recorded and the exothermic enthalpy of refreezing (ΔH_r) was calculated. THA was calculated using Eq. (3):

$$\mathrm{THA} = T_h - T_0 \tag{3}$$

where T_h was the holding temperature, and T_0 was the onset temperature when the exothermic process began.

The fraction of ice (Φ) in the sample was then estimated using Eq. (4):

$$\Phi\,(\%) = (1 - \frac{\Delta H_r}{\Delta H_m}) \times 100 \quad (4)$$

where ΔH_r is the exothermic enthalpy of refreezing at Th temperature, and ΔH_m is the enthalpy of melting.

The above experimental procedure was repeated with different hold temperatures to obtain different partially melted systems with varying ice-contents.

2.6. Determination of ice structuring activity

The ice structuring activity of sericin peptides was assessed using a polarising optical microscope with a cold stage (Leica DM LP, Leica Microsystems GmbH, Germany) based on previous protocols with minor modifications (Wang & Damodaran, 2009). In a typical experiment, a small drop (3 μl) of 36% (w/w) sucrose solution (with or without sericin peptides) was placed between two circular 10 mm glass cover slips, which were pressed together to produce a sample film. The glass slide was placed inside the cold storage, and both the interior and upper window of the cold stage were purged with dry nitrogen to prevent the condensation of ambient water vapour. The glass slide was frozen quickly by decreasing the temperature from ambient to −50 °C at rate of −20 °C/min. It was then held at −50 °C for 1 min, and a microscopic image of the sample at −50 °C was recorded. The temperature of the sample was then increased gradually from −50 to −14 °C at the rate of 5 °C/min, held at −14 °C for 1 min, and then cycled 5 times between −14 and −12 °C at a rate of 1 °C/min. Ice crystal growth was monitored and photographed at the end of the 5 cycles through cross-polarising lenses.

2.7. Peptide sequence analysis by UPLC–ESI-TOF/MS

Separated fractions with the highest antifreeze activity were characterised, using an ultra performance liquid chromatography–positive ion electrospray-time of flight mass spectrometer (UPLC–ESI-TOF/MS, Waters Company, Milford, Massachusetts, USA). As peptides eluted from the column into the mass spectrometer, peptides with high abundance and selectivity for quantification were selected and analysed by ESI-TOF/MS, before the molecular mass was analysed and sequence was inferred using the De Novo Explorer software.

LC analysis was performed, using a Waters Acquity UPLC system coupled to a Waters Acquity PDA detector. One microlitre of sample was loaded onto a BEH C18-MS column (2.1 mm × 100 mm, 1.7 μm), eluted in a linear gradient of 10–90% acetonitrile solution for 20 min at a flow rate of 0.3 ml/min at 50 °C, and detected using a UV detector which was set in the range of 200–600 nm.

MS analysis was performed using a Waters SYNAPT QTF MS system. The parameters for the analysis were as follows: reflector, positive; mass range, 50–2000 m/z; ESI source temperature, 100 °C; desolvation temperature, 250 °C; capillary voltage, 3.5 kV; photomultiplier tube voltage, 1600 V.

2.8. Antifreeze peptide synthesis and purification

The peptide with the highest antifreeze activity was synthesized by F-moc chemistry (Fields & Noble, 1990) on a glass reaction column peptide synthesizer (BZ24/29, D = 250 mm Singapore Glass Instrument Factory). It was then purified by HPLC (Shimadzu LC-10AVP HPLC system) on a reversed phase C-18 (4.6 mm × 250 mm) column, using solvent gradient (A: 0.1% (v/v) TFA in H_2O; B: 0.1% (v/v) TFA in CH_3CN) to a purity of at least 95%. The sequence was then confirmed by analysis with a Waters Micromass ZQ 2000 LC/MS mass spectrometer. Dry synthetic peptide purified by HPLC was stored at −20 °C, dissolved immediately in sterile water to a final concentration of 100 μg/ml, and used in experiments to analyse its hypothermia protective activities.

2.9. Peptide concentration determination

The concentration of sericin peptides used in the above experiments was determined by the method of Lowry (Lowry, Rosebrough, Farr, & Randall, 1951) using bovine serum albumin as a standard.

2.10. Molecular modelling of the ice-binding action

Construction of the peptide/ice binding model was performed with the antifreeze peptide on the (2 0 1) plane of ice, using the Accelrys Materials Studio v4.4 programme. The ice had a hexagonal structure with a P63/mmc space group, and the unit cell constants were $a = b = 4.516$ Å, $c = 7.354$ Å, $\alpha = \beta = 90°$, $\gamma = 120°$ (Madura et al., 1996). The sericin antifreeze peptide was placed onto the ice (2 0 1) surface. The ice slab consisted of 2295 water molecules, and its dimensions were $46.16 \times 40.64 \times 40.70$ Å^3.

The SPC (single point charge) model was used for the ice phase of water, and COMPASS force field (Sun, 1998) was used for both the peptide and the ice-slab. Electrostatic interactions were evaluated by using the Ewald summation technique, and van der Waals interactions were switched off at 12.5 Å.

The interaction strength of the (2 0 1) surface of ice with the peptide could be shown by the binding energy, which was calculated by expression 5:

$$E_{binding} = E_{complex} - (E_{peptide} + E_{ice}) \quad (5)$$

where $E_{complex}$ is the total energy of the peptide/ice system, $E_{peptide}$ was the energy of the sericin antifreeze peptide, and E_{ice} is the energy of the ice slab.

The peptide/ice system was minimised by smart algorithm with ice oxygen atoms fixed in their crystal positions, and others being free to move. The peptide was translated along the x-direction to obtain the lowest energy system. The final configuration of the lowest energy system was subjected to a NVT dynamics simulation of 300 ps at 165 K without constraints imposed on the system. The binding energy was then calculated as described above.

2.11. Statistical analyses

All experiments were conducted in triplicate, or double, and all data are presented as means (standard deviations, SDs) of three independent experiments or mean of two independent experiments. Statistical analysis was performed using the Student's t-test, and a value of $p < 0.05$ was considered to be statistically significant.

3. Results and discussion

3.1. Thermal hysteresis activity of ice-binding sericin peptides

The sericin peptides were previously proved to have specific ice-binding ability, and also exerted obvious hypothermia protective effects on *L. bulgaricus LB340* in a cold environment (Wu et al., 2013). In this study, DSC was used to further study the thermal hysteresis activity of I-SP. DSC curves of the freezing and melting processes for BSA, SP (original hydrolysed sericin peptides), and I-SP solutions are shown in Fig. 1a. The calculated thermal hysteresis activities (THAs) and ice fractions (Φ) at different T_h, based on the DSC curves were plotted and are shown in Fig. 1b and c, respectively.

In the control experiment, recrystallisation of the melted portion started immediately after the temperature dropped, and the exothermic peak appeared without delay (Fig. 1aI). This indicated that BSA solution, a non-antifreeze standard protein, had no thermal hysteresis activity. However, compared with the DSC curves of BSA, a delayed onset of refreezing temperature (T_0) was observed for I-SP, with an increase from −0.67 to −1.24 °C as the T_h increased from −0.40 °C (m curve) to −0.30 °C (n curve). This suggests that the I-SP solution displayed some thermal hysteresis properties (Fig. 1aIII).

Furthermore, the data shown in Fig. 1b indicate that the amount of ice nuclei (Φ) in the equilibrium sample decreased accordingly from 49.28% to 1.16% with rising T_h, from −0.59 to −0.19 °C. However, with less ice fraction in the equilibrium sample, higher THA

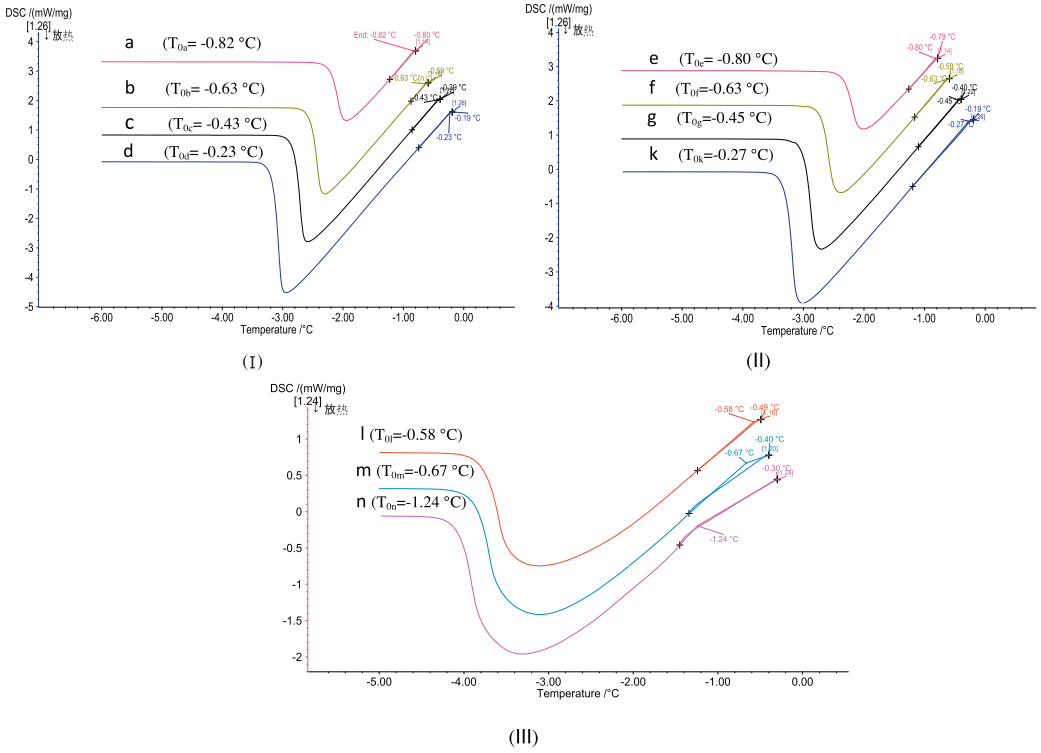

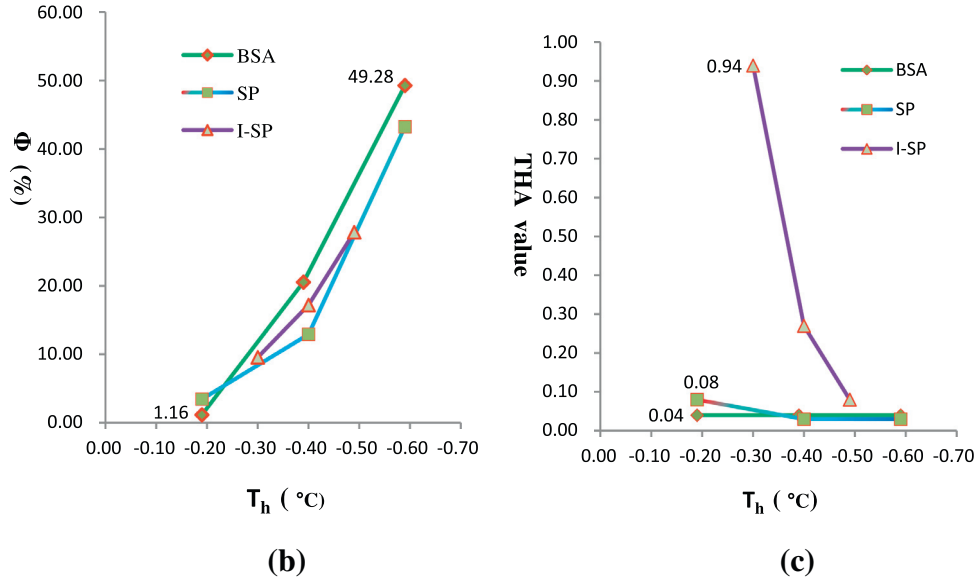

Fig. 1. The thermal hysteresis activity (THA) of ice-binding sericin peptides (I-SP) compared to SP (original hydrolysed sericin peptides), as well as the negative control of BSA (AFP-free protein). (a) The differential scanning calorimetry (DSC) typical curves of the freezing and melting processes at different hold temperature (T_h) temperatures for (I) BSA, (II) SP and (III) I-SP. The T_h values of the curves from curve a to curve d in (I) were −0.80, −0.59, −0.39, and −0.19 °C, respectively. The T_h values of the curves e to k in (II) was −0.79, −0.59, −0.40, and −0.19 °C, respectively. The T_h values of the curves l to n in (III) was −0.49, −0.40, and −0.30 °C, respectively. The T_0 value of each curve is in parentheses. Ice fraction (Φ)–T_h plots of SP (■), I-SP (▲) and BSA (♦). Data points represent mean values calculated from two separate experiments. (b) THA-Th plots of SP (■), I-SP (▲) and BSA (♦). Data points represent mean values calculated from two separate experiments.

values were obtained. When the ice fraction was less than 10%, the THA value of SP and I-SP increased to 0.08 and 0.94 °C, respectively; however, the THA value of BSA was only 0.04 °C, lower than those of SP and I-SP (Fig. 1c).

In addition, the THA of ApAFP752 from the desert beetle, *Anatolica polita,* was reported to reach as high as 0.76 °C when the amount of ice in the solution was less than 5.1% (Mao, Liu, Li, Ma, & Zhang, 2011). Thus, the THA of I-SP obtained in this study was higher than the THA of the insect antifreeze protein, ApAFP752, obtained during similar freezing and melting processes. Moreover, previous reports have demonstrated that the THA of AFPs from insects was ~5–6 °C, that of fish was 1.0–1.5 °C, and that of plants was 0.1–0.45 °C (Jia et al., 2012). Therefore, the THA of the I-SP derived from silkworm was higher than that from plants, but lower than other insect AFPs.

3.2. Isolation of high activity antifreeze sericin peptides

The extracted I-SP was then loaded onto a C18 reversed-phase high performance liquid chromatography preparative column, and the elution profile is shown in Fig. 2a. Data revealed that the I-SP was separated mainly into four chromatographic peaks, and six different fractions were collected from the column, based on the elution profile. Fractions were then pooled and freeze-dried for further hypothermia protection activity (HPA) analyses.

After a 24 h cold treatment, the survival of *L. bulgaricus LB340* cells with added sterilised water as a control was relatively low, whereas the survival of cells to which the P1 to P6 fractions were added was higher than that of the water control, and significantly higher than that of the glycerol-treated positive control (Fig. 2b).

The P4 fraction displayed the highest HPA of all the fractions, and had >2.9- and 1-fold higher HPA compared with the sterilised water and glycerol controls, respectively (Fig. 2b). Furthermore, the ice-structuring activity of the P4 fraction for the inhibition of ice recrystallisation was determined using a polarising optical microscope with a cold stage (Fig. 2c). It should be noted that the ice crystals in the control solutions without the P4 fraction were large and circular in shape (Fig. 2cII) because the ice/liquid interface energy was minimised in this geometry, and the Ostwald ripening process facilitated the growth of ice crystals during the five cycles of −14 to −12 °C. In contrast, ice crystals in the presence of the P4 fraction were smaller with an irregular shape (Fig. 2cIV), suggesting that there was a specific interaction between the ice and the sericin antifreeze peptides that reduced the Ostwald ripening process by adsorbing the effectors (such as ice-structuring peptides) to the faces of ice crystal faces (Heggemann et al., 2010). These data clearly revealed that the P4 fraction had strong antifreeze activity since it enhanced the survival of *L. bulgaricus LB340* strain cells significantly after 24 h cold treatment and inhibited ice recrystallisation.

3.3. Synthesis and characterisation of a novel antifreeze sericin peptide from the P4 fraction

The P4 fraction that demonstrated strong antifreeze activity was separated by UPLC, followed by detection with ESI-TOF-MS. Fig. 2d shows a typical mass chromatogram and mass spectra of the P4 fraction obtained from TOF-MS analysis with positive ion mode (ESI+). Data suggested that the P4 fraction was a homogeneous component eluted on the C18 reversed chromatographic column, and that it contained few impurities (Fig. 2dI). As shown in Fig. 2dII, peptide ion M, eluted at a retention time of 7.08 min, had the highest abundance and highest resolution of all the ions. A clean MS spectrum was obtained from peptide ion M (Fig. 2dIII), and some a-, b- and y-ions derived from the peptide ion M are also shown. De Novo Explorer software and the electrospray ionisation-principles and practice, demonstrated that peptide ion M was a peptide with a molecular mass of 1009.50 Da, and its structure was inferred to be TTSPTNVSTT. The theoretical molecular weight of the inferred peptide (named as a novel sericin antifreeze peptide M, SM-AFP) was calculated as 1010 Da, using online peptide molecular weight calculation software (http://www.biopeptide.com/PepCalc/Calculate), which was consistent with the molecular weight of peptide ion M detected by MS.

To confirm the accuracy of the SM-AFP primary sequence and assess its corresponding HPA, SM-AFP was synthesized, using the Fmoc solid phase synthetic method. The synthetic product was chromatographed by HPLC, and the only homogeneous shape throughout an elution peak in the chromatogram meant that it was a homogeneous peptide component, as shown in Fig. 3a. The molecular weight of SM-AFP was then determined by LC/MS from the peak corresponding to the singly and multiply protonated intact molecule. Fig. 3b shows that the singly protonated intact molecule $[M+H]^+$ was 1008.70 m/z and the multiply protonated intact molecule $[M+K+H]^{2+}$ was 505.10 m/z. This resulted in a measured relative molecular weight of SM-AFP of 1009.7 Da, which was consistent with the molecular weight determined by mass spectrometry. Therefore, these data provided a valuable initial verification of the accuracy of the synthesized sequence.

The synthetic SM-AFP was analysed further by assessing its HPA. The mean survival of *L. bulgaricus LB340* in the sterile water control was 11.11%, whereas the mean survival of *L. bulgaricus LB340* treated with 100 μg/ml of synthetic SM-AFP was 26.90%, i.e., an approximately 1.4-fold increase compared with water control ($p < 0.05$) (Fig. 3c). These data suggest that the pure SM-AFP obtained in this study was a novel antifreeze peptide derived from silkworm AFP. It may have potential to be utilised as a probiotic hypothermia protectant.

3.4. Molecular modelling of the interface binding of SM-AFP on ice

To our knowledge, there is no direct experimental way to investigate the molecular interactions between AFPs and growing ice crystals, which are important for understanding the mechanism of the antifreeze activity of AFPs. Over the past decade, molecular dynamics simulations were efficiently employed to characterise AFP structures and their interactions with ice planes, predominantly at the ice/vacuum interface or in the water/ice system (Cheng et al., 2002; Madura, Baran, & Wierzbicki, 2000). In this study, we used an SM-AFP/ice vacuum system as the object without considering the effect of the water phase to simplify the simulation process. The optimised molecular structure of SM-AFP, with the sequence Thr-Thr-Ser-Pro-Thr-Asn-Val-Ser-Thr-Thr ($T_1T_2S_3P_4$-$T_5N_6V_7S_8T_9T_{10}$), is shown in Fig. 4a. To study the interaction between SM-AFP and ice, hydrogen bonds were calculated. The cut-off for a hydrogen bond donor–acceptor distance and donor–hydrogen-acceptor angle were 2.5 Å and 90°, respectively.

The peptide was placed on the (2 0 1) surface of ice, which was translated along the *x*-direction and ten different conformations were obtained. Their total energies for each conformation were separately calculated and the lowest energy system was obtained, the final configuration of which is depicted in Fig. 4b. The total number of hydrogen bonds for SM-AFP and the (2 0 1) surface of ice was 13; four were intra-molecular hydrogen bonds in SM-AFP, and nine were intermolecular hydrogen bonds between SM-AFP and the ice surface (Fig. 4c). The hydrogen bonding of SM-AFP to the (2 0 1) surface of ice occurred predominantly via threonine and asparagine residues, since five hydrogen bonds were established between threonine and the ice surface, and three were formed between asparagine and the ice surface (Table 1). It should also be noted that the hydrophilic side chains of Thr (T_1, T_2, T_5, T_9) and Asn not only faced the ice surface and formed multiple hydrogen bonds with O or H

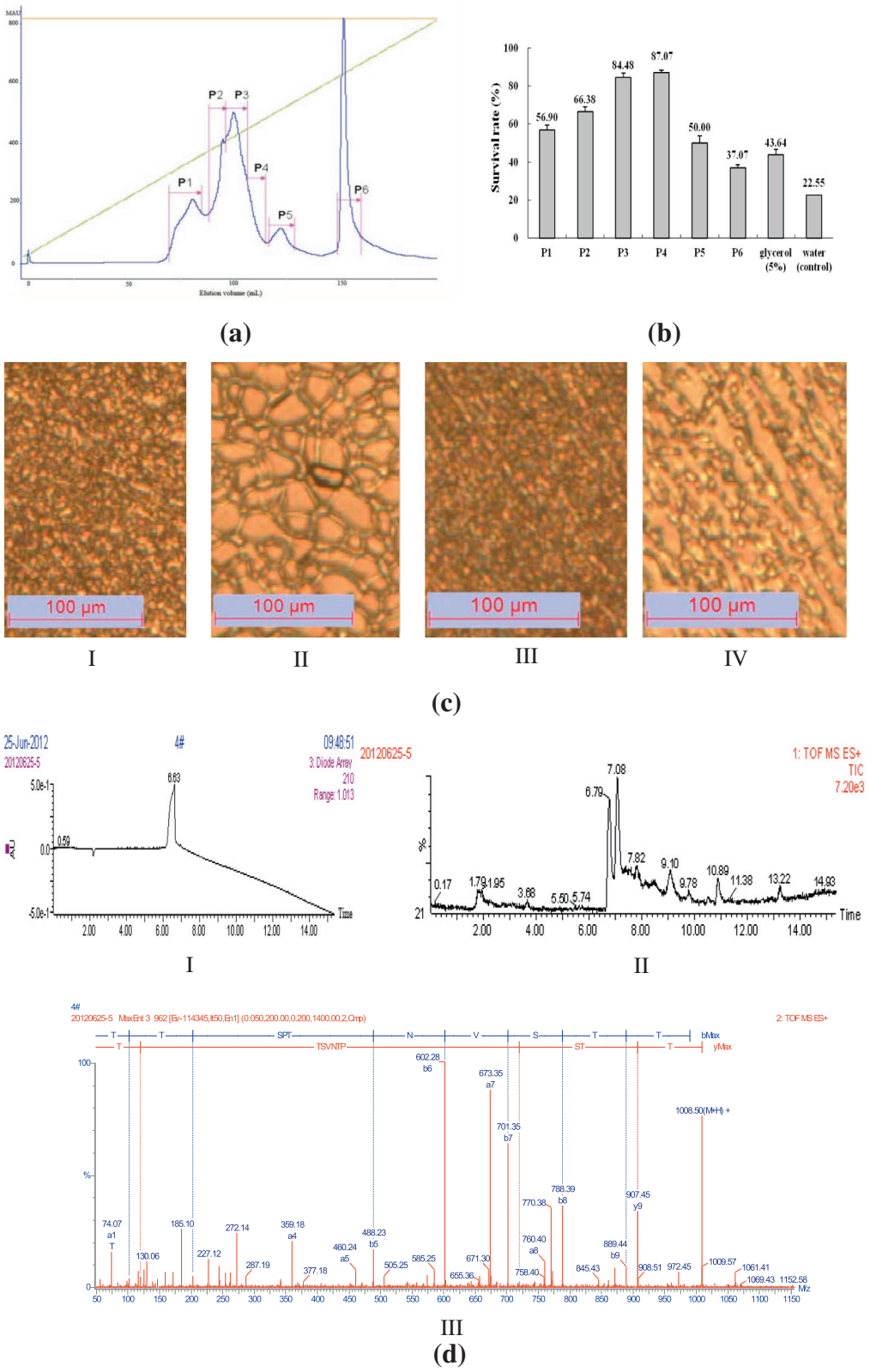

Fig. 2. Isolation of a novel sericin antifreeze peptide from I-SP. (a) Elution profile of I-SP on a C18 reversed phase chromatographic column (25 mm diameter × 250 mm length) in a fast protein liquid chromatography system with a flow rate of 10 ml/min and a UV detector at 220 nm. The locations of the different fractions (P) are shown. (b) The hypothermia protective effects of fractions (P1–P5) eluted from a C18 reversed phase high performance liquid chromatography preparative column on *L. bulgaricus LB340* stored at −20 °C for 24 h. Sterile water and 5% (v/v) glycerol were used as the negative and positive controls, respectively. (c) The effect of fraction P4 on ice crystal growth in 36% (wt) sucrose solution without fraction P4 before (I) and after (II) five cycles of −14 to −12 °C, and (III) and (IV) show 36% (wt) sucrose solution with 1 mg/ml of fraction P4 addition before and after 5 cycles at −14 to −12 °C, respectively. (d) High performance liquid chromatogram (I) and TIC spectrogram (II) of the P4 fraction analysed by UPLC–ESI-TOF-MS in positive ion mode. MS spectrum of the peptide ion (M), which had the highest abundance and a high resolution, eluted at 7.08 min in the TIC spectrogram is shown (III), and some a-, b- and y-ions derived from the peptide ion are also shown.

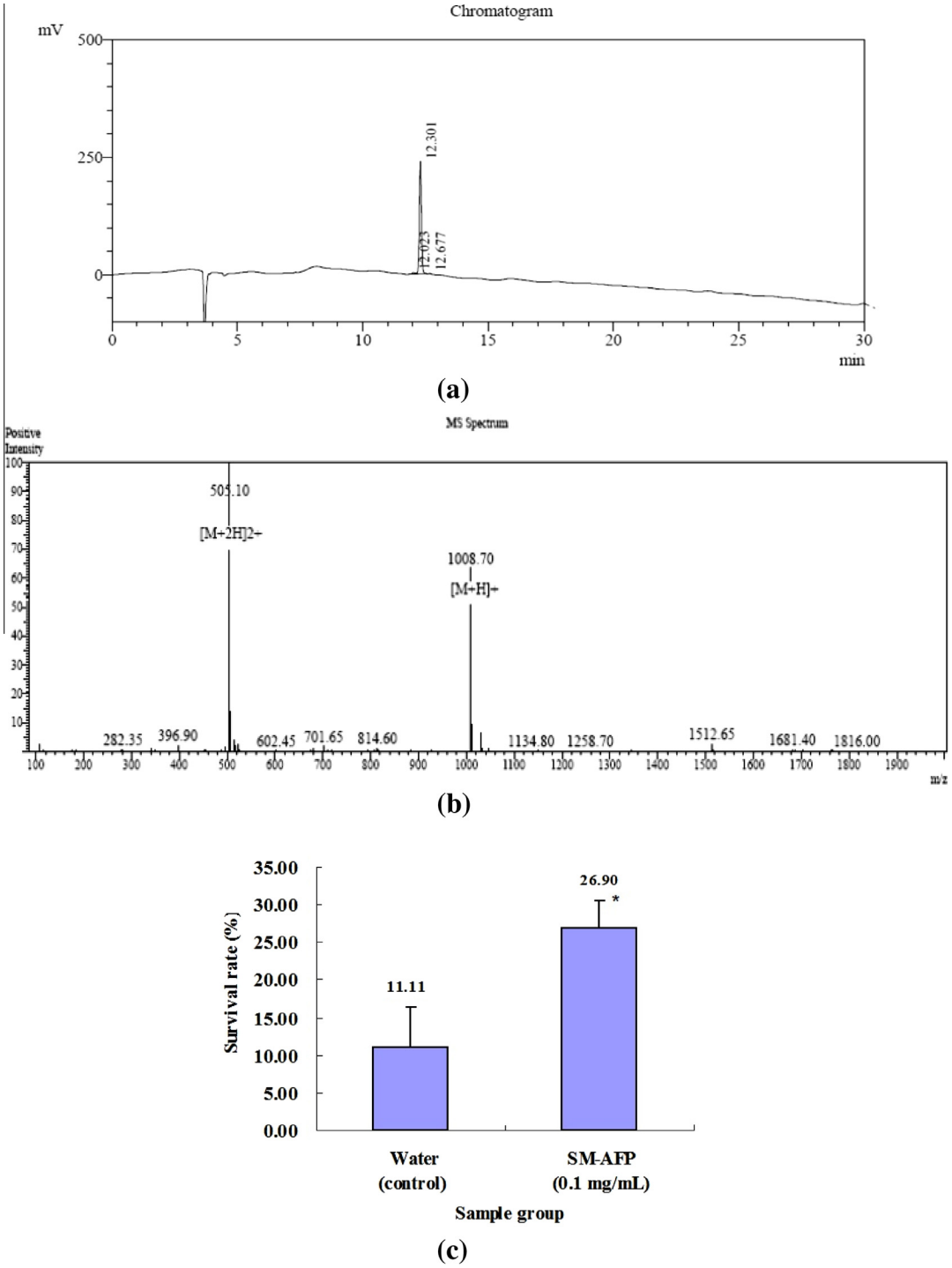

Fig. 3. Characterisation of synthetic SM-AFP by HPLC, LC/MS and analysis of its hypothermia protective activity. (a) Chromatogram of synthetic SM-AFP, which was eluted using solvent gradients [A, 0.1% (v/v) TFA in H_2O; B, 0.1% (v/v) TFA in CH_3CN]. A linear gradient of solvent B at 2–65% for 30 min was then carried out at a flow rate of 1 ml/min at room temperature, and the detector was set at 214 nm. (b) Mass spectrum of the synthetic SM-AFP. Electrospray ionisation was performed, and the other parameters were as follows: elution buffer, 50% H_2O/50% methanol; flow rate, 0.2 ml/min; CDL temperature, 250 °C; nebulizing gas flow, 1.50 l/min; pre-rod bias, +4.5 kv; detector, −0.2 kv. Mass spectra were recorded in positive ion mode in m/z. (c) The hypothermia protective effect of 100 μg/ml of synthetic SM-AFP on *L. bulgaricus LB340* at −20 °C storage over 24 h. Sterile water was used as a negative control.

atoms of ice surface, but the side chains also sat on the ridges of the ice surface (Fig. 4c). This finding was consistent with the results reported by Wen and Laursen (1993), who reported that the protein face consisting of Thr and Asx residues interacted with the ice. The lengths and angles of hydrogen bonds formed between SM-AFP and ice are summarised in Table 2. Generally, hydrogen bonds formed between H and A with distances less than 2 Å awwre considered to be very strong. Therefore, the strongest hydrogen bonds were predominantly the NH—O and OH—O interactions, formed by the amino or hydroxyl atoms of Thr and Asn residues with oxygen atoms on the ice surface. During energy minimisation, the ice-binding residues underwent significant conformational changes, where the main chain amino group of T_1 and the side chain hydroxyl group of T_9 bent towards the ice surface. These changes suggest that the ice

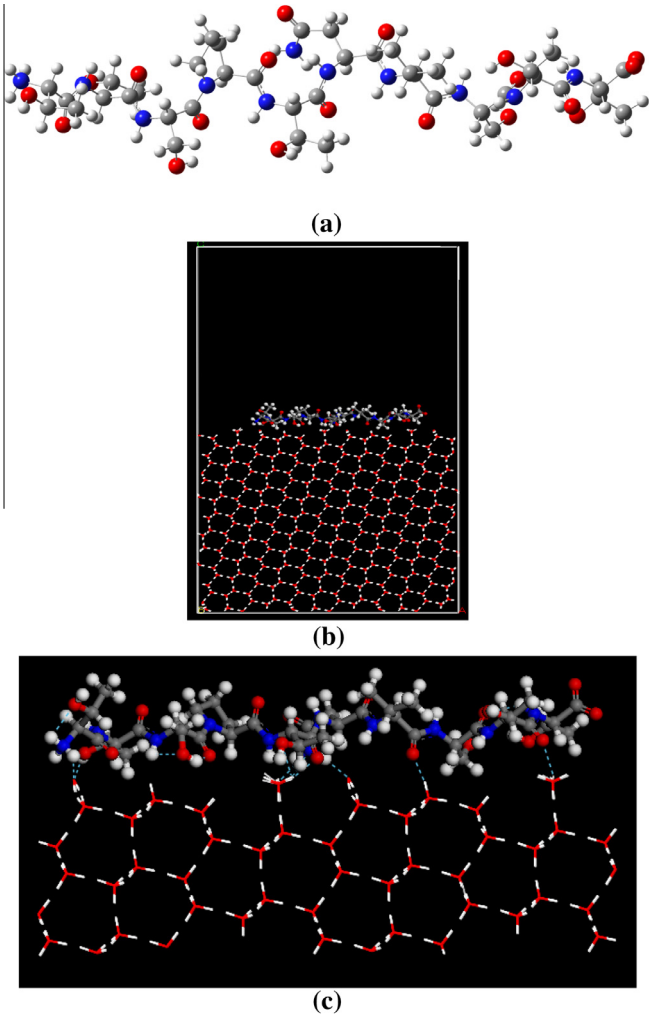

Fig. 4. The optimised molecular structure of SM-AFP shown in a ball and stick model (a), snapshot of the lowest energy ice/SM-AFP system (b) and interception of the surface area of the ice/SM-AFP system (c). Red, blue, grey and white balls represent oxygen, nitrogen, carbon, and hydrogen atoms, respectively, and blue dashed lines represent hydrogen bonds. (For interpretation of the references to colour in this figure legend, the reader is referred to the web version of this article.)

Table 1
Summary of the intermolecular hydrogen bonds formed between SM-AFP and ice.

Number of hydrogen bonds	SM-AFP		Atoms of water molecules of ice plane
	Amino acid residues	Atoms (groups)	
1	$\mathbf{T}_1$ (N-terminal)	H (amino)	O
1	$\mathbf{T}_2$	H (hydroxyl)	O
2	$\mathbf{T}_5$	O (hydroxyl)	H
		O (carbonyl)	H
1	$\mathbf{T}_9$	O (carbonyl)	H
3	$\mathbf{N}_6$	N (amino)	H
		N (amino)	H
		H (amino)	O
1	$\mathbf{V}_7$	O (carbonyl)	H

environment did not impose a steric restriction on the Thr and Asn side chains. Cheng et al. (2002) demonstrated that the hydrogen bonds in an ice lattice would be broken upon interaction with AFP by a slightly twisted lattice or distorted ice surface layers, which resulted in a partial melting of the surface of an ice crystal that prevented it from further growth.

Table 2
Lengths (d) and angles ($\angle$) of hydrogen bonds formed between SM-AFP and ice.

D—H···A	d (H···A) (Å)	d (D···A) (Å)	∠DHA (°)
T_1:N—H···O	1.655	2.555	145.3
T_2:O—H···O	1.691	2.519	141.0
O—H···O:T_5	2.111	2.410	96.2
O—H···O:T_5	1.672	2.612	163.6
O—H···O:T_9	2.265	2.977	130.6
O—H···N:N_6	2.435	2.799	102.42
O—H···N:N_6	2.406	2.799	104.30
N_6:N—H···O	1.765	2.769	171.5
O—H···O:V_7	1.723	2.654	161.4

In this study, the hydrophobic side chains of proline and valine faced away from the ice surface (Fig. 4c). Consistent with this, Kim et al. (2009) suggested that the presence of proline residues impeded the incorporation of the peptide itself and other water molecules into the ice crystal near the peptide-binding site, which resulted in the kinetic inhibition of crystal growth. The hydrophobic interaction was studied mostly in the ice/water/AFP system (Haymet, Ward, & Harding, 1999). This suggests that the SM-AFP/ice/vacuum simulations used in this study were inadequate, and that future studies using SM-AFP/ice/water simulations are necessary to obtain a more thorough understanding of the ice binding mechanism of SM-AFP.

In addition, non-bond interactions, e.g. van der Waals and Coulomb, were also a major source of ice-AFP interactions (Dalal & Sonnichsen, 2000). After energy minimisation, the lowest energy system was subjected to molecular dynamics simulation. Chen and Jia (1999) have reported the binding of fish type III antifreeze protein and ice, in which a 120 ps simulation time was used and the systems were fully equilibrated. In this study, 300 ps simulation time was performed to fully confirm the equilibration. As a result, the energy and temperature reached a plateau after a 300 ps simulation, so this simulation by molecular dynamics was judged to be fully equilibrated. The total energy of ice/SM-AFP, the ice slab, and SM-AFP was calculated separately. According to Eq. (5), the binding energy was calculated to be -143.0 kcal mol^{-1}, and this energy value meant that the interaction of ice/SM-AFP was exothermic and SM-AFP was bound irreversibly to the ice. Since Wierzbicki, Madura, Salmon, and Sonnichsen (1997) reported the binding of sea raven AFP to the ice surface with a binding energy of -302 kcal mol^{-1}, we could conclude that there was a strong binding of the SM-AFP to the (201) surface of the ice, and non-bond interactions also contributed to the binding of SM-AFP with the ice surface.

4. Conclusion

This study focussed on the isolation and characterisation of a purified sericin antifreeze peptide derived from I-SP, and performed molecular modelling of the interface binding between the purified sericin antifreeze peptide and the (201) surface of ice. Results demonstrated that I-SP exhibited obvious THA. A P4 fraction, obtained from the I-SP, displayed high HPA, as well as ice structuring activity, to inhibit ice recrystallisation. SM-AFP, a novel antifreeze sericin peptide with a molecular mass of 1009.50 Da and sequence of TTSPTNVSTT, was isolated from the P4 fraction, and exerted obvious HPA in *L. bulgaricus LB340*. Furthermore, molecular modelling of the interface binding of SM-AFP to the (201) surface of ice suggested that the adsorption of SM-AFP to the ice crystal surface and prevention of ice crystal growth could be attributed partially to hydrogen bonds between threonine and asparagine residues and the atoms of ice phase water; hydrophobic interaction resulted from the hydrophobic side chains of proline and

valine, as well as non-bond interactions including van der Waals and Coulomb. These findings suggested that sericin peptides are novel antifreeze molecules derived from *Lepidoptera* insects, and that SM-AFP, which exhibits a strong ice-binding activity, could be used as a beneficial additive to probiotics or other processed foods that require low temperature storage.

Acknowledgements

The authors thank the National Natural Science Foundation of China for financial supports (No. 31471623, No. 31000814, No. 31071498, No. 31171642). This research was also funded partly by the Natural Science Foundation of Fujian Province of China (No. 2013J01132), and the Medical-Engineering Cross Project with Grant YG2011MS64, which is financially supported by Shanghai Jiao Tong University, China.

References

Chen, G. J., & Jia, Z. (1999). Ice-binding surface of fish Type III antifreeze. *Biophysical Journal, 77*, 1602–1608.

Cheng, C. H. C. (1998). Evolution of the diverse antifreeze proteins. *Current Opinion in Genetics & Development, 8*(6), 715–720.

Cheng, Y., Yang, Z., Tan, H., Liu, R., Chen, G., & Jia, Z. (2002). Analysis of ice-binding sites in fish Type II antifreeze protein by quantum mechanics. *Biophysical Journal, 83*, 2202–2210.

Dalal, P., & Sonnichsen, F. D. (2000). Source of the ice-binding specificity of antifreeze protein Type I. *Journal of Chemical Information and Modeling, 40*, 1276–1284.

Danks, H. V. (2004). The roles of insert cocoons in cold conditions. *European Journal of Entomology, 101*, 433–437.

Fields, G. B., & Noble, R. L. (1990). Solid-phase peptide synthesis utilizing 9-fluorenylmethoxycarbonyl amino acids. *International Journal of Peptide and Protein Research, 35*, 161–214.

Graether, S. P., Gagné, S. M., Spyracopoulos, L., Jia, Z. C., Davies, P. L., & Sykes, B. D. (2003). Spruce budworm antifreeze protein: Changes in structure and dynamics at low temperature. *Journal of Molecular Biology, 327*, 1155–1168.

Graham, L. A., Qin, W., Lougheed, S. C., Davies, P. L., & Walker, V. K. (2007). Evolution of hyperactive, repetitive antifreeze proteins in beetles. *Journal of Molecular Evolution, 64*, 1–13.

Harding, M. M., Anderberg, P. I., & Haymet, A. D. J. (2003). Antifreeze glycoproteins from polar fish. *European Journal of Biochemistry, 270*, 1381–1392.

Hassas-Roudsari, M., & Goff, H. D. (2012). Ice structuring proteins from plants: Mechanism of action and food application. *Food Research International, 46*, 425–436.

Haymet, A. D., Ward, L. G., & Harding, M. M. (1999). Winter flounder "antifreeze" proteins: synthesis and ice growth inhibition of analogues that probe the relative importance of hydrophobic and hydrogen-bonding interactions. *Journal of the American Chemical Society, 121*, 941–948.

Heggemann, C., Budke, C., Schomburg, B., Majer, Z., Wißbrock, M., Koop, T., et al. (2010). Antifreeze glycopeptide analogues: Microwave-enhanced synthesis and functional studies. *Amino Acids, 38*, 213–222.

Jia, C., Huang, W., Wu, C., Lv, X., Rayas-Duarte, P., & Zhang, L. (2012). Characterization and yeast cryoprotective performance for thermostable ice-structuring proteins from Chinese Privet (*Ligustrum Vulgare*) leaves. *Food Research International, 49*, 280–284.

Kawahara, H. (2002). The structures and functions of ice crystal controlling proteins from bacteria. *Journal of Bioscience and Bioengineering, 94*(6), 492–496.

Kim, J. S., Damodaran, S., & Yethiraj, A. (2009). Retardation of ice crystallization by short peptides. *The Journal of Physical Chemistry A, 113*, 4403–4407.

Lowry, O. H., Rosebrough, N. J., Farr, A. L., & Randall, R. J. (1951). Protein measurement with the folin phenol reagent. *Journal of Biological Chemistry, 193*, 265–275.

Madura, J. D., Baran, K., & Wierzbicki, A. (2000). Molecular recognition and binding of thermal hysteresis proteins to ice. *Journal of Molecular Recognition, 13*, 101–113.

Madura, J. D., Taylor, M. S., Wierzbicki, A., Harrington, J. P., Sikes, C. S., & Sonnichsen, F. (1996). The dynamics and binding of a Type III antifreeze protein in water and on ice. *Journal of Molecular Structure (Theochem), 388*, 65–77.

Mao, X. F., Liu, Z. Y., Li, H. L., Ma, J., & Zhang, F. C. (2011). Calorimetric studies on an insect antifreeze protein ApAFP752 from *Anatolica polita*. *Journal of Thermal Analysis and Calorimetry, 104*, 343–349.

Qin, W. S., & Walker, V. K. (2006). Tenebrio molitor antifreeze protein gene identification and regulation. *Gene, 367*, 142–149.

Sun, H. (1998). COMPASS: An ab initio forcefield optimized for condensed-phase applications-overview with details on alkane and benzene compounds. *Journal of Physical Chemistry B, 102*, 7338–7364.

Tsujimoto, K., Takagi, H., Takahashi, M., Yamada, H., & Nakamori, S. (2001). Cryoprotective effect of the serine-rich repetitive sequence in silk protein sericin. *The Journal of Biochemistry, 129*, 979–986.

Venketesh, S., & Dayananda, C. (2008). Properties, potentials, and prospects of antifreeze proteins. *Critical Reviews in Biotechnology, 28*, 57–82.

Wang, S. Y., & Damodaran, S. (2009). Ice-structuring peptides derived from bovine collagen. *Journal of Agricultural and Food Chemistry, 57*, 5501–5509.

Wen, D., & Laursen, R. A. (1993). Structure-function relationships in an antifreeze polypeptide: The effect of added bulky groups on activity. *The Journal of Biological Chemistry, 268*, 16401–16405.

Wierzbicki, A., Madura, J. D., Salmon, C., & Sonnichsen, F. (1997). Modeling studies of binding of sea raven Type II antifreeze protein to ice. *Journal of Chemical Information and Modeling, 37*, 1006–1010.

Wu, J. H., Wang, S. Y., Wu, Y., & Wang, Z. W. (2012). Cryoprotective effect of sericin enzymatic peptides on the freeze-induced denaturation of grass carp surimi. *Applied Mechanics and Materials, 140*, 291–295.

Wu, J. H., Zhou, Y. H., Wang, S. Y., Wang, Z. W., Wu, Y., & Guo, X. Q. (2013). Laboratory-scale extraction and characterization of ice-binding sericin peptides. *European Food Research and Technology, 236*, 637–646.

Xiao, N., Suzuki, K., Nishimiya, Y., Kondo, H., Miura1, A., Tsuda, S., et al. (2010). Comparison of functional properties of two fungal antifreeze proteins from *Antarctomyces psychrotrophicus* and *Typhula ishikariensis*. *FEBS Journal, 277*, 394–403.

Zhang, C., Zhang, H., Wang, L., Zhang, J. H., & Yao, H. Y. (2007). Purification of antifreeze protein from wheat bran (*Triticum aestivum* L.) based on its hydrophilicity and ice-binding capacity. *Journal of Agricultural and Food Chemistry, 55*, 7654–7658.